atmosphere

MDPI

Article

Different Effects of a Super Storm on Atmospheric Electric Fields at Different Latitudes

Wen Li [1,2], Zhibin Sun [1,*], Tao Chen [1], Zhaoai Yan [1,*], Jing Luo [1], Qingchen Xu [1] and Zhongsong Ma [3]

[1] State Key Laboratory of Space Weather, National Space Science Center, Chinese Academy of Sciences, Beijing 100190, China; liwen@nssc.ac.cn (W.L.); tchen2024@proton.me (T.C.); jluo@swl.ac.cn (J.L.); xqc@nssc.ac.cn (Q.X.)
[2] University of Chinese Academy of Sciences, Beijing 100049, China
[3] Technology and Engineering Center for Space Utilization, Chinese Academy of Sciences, Beijing 100094, China; mazhongsong@csu.ac.cn
* Correspondence: zbsun@nssc.ac.cn (Z.S.); yanza@126.com (Z.Y.); Tel.: +86-13810195052 (Z.S.); +86-15810330687 (Z.Y.)

Abstract: Geomagnetic storms have a significant impact on Earth's magnetosphere and ionosphere, as well as on the global atmospheric circuit. This study focuses on investigating the anomalous variations in the vertical atmospheric electric field at eight mid-latitude and low-latitude stations during a mega-geomagnetic storm on 24 April 2023. The majority of stations observed vertical atmospheric electric field increases, while only three nearby stations exhibited vertical atmospheric electric field decreases. The analysis revealed that vertical atmospheric electric field changes ranged from 19 to 370 V/m, and the time differences between extreme vertical atmospheric electric field values and the minimum Dst value ranged from 0 to 5.3 h. Other response patterns to this super magnetic storm at different latitudes are summarized, and the physical mechanisms of different effects of magnetic storms on the electric fields of stations at different latitudes are also discussed.

Keywords: super storm; different latitudes; atmospheric electric field

check for updates

Citation: Li, W.; Sun, Z.; Chen, T.; Yan, Z.; Luo, J.; Xu, Q.; Ma, Z. Different Effects of a Super Storm on Atmospheric Electric Fields at Different Latitudes. *Atmosphere* **2024**, *15*, 1314. https://doi.org/10.3390/atmos15111314

Academic Editor: Christine Amory-Mazaudier

Received: 6 October 2024
Revised: 23 October 2024
Accepted: 23 October 2024
Published: 31 October 2024

Copyright: © 2024 by the authors. Licensee MDPI, Basel, Switzerland. This article is an open access article distributed under the terms and conditions of the Creative Commons Attribution (CC BY) license (https://creativecommons.org/licenses/by/4.0/).

1. Introduction

The vertical atmospheric electric field (Ez) is the electric field that exists between the bottom of the ionosphere and the Earth's surface, and its magnitude is equal to the atmospheric potential gradient at a certain point. It is critical to understand the global atmospheric circuit to investigate Ez variations, and the "global circuit hypothesis" was conceived by Wilson [1]. Over the past few years, there has been a growing interest in the study of the global atmospheric circuit, both in terms of observations and modeling [2,3]. For the global atmospheric circuit, the total column resistance is 200 Ω. For thunderstorms, electrified shower clouds and precipitation act as batteries for the circuit, with the current carried by cluster ions generated by radioactivity and galactic cosmic rays. Solar activities affect the global atmospheric circuit through the modulation of particle precipitation, X-ray bremsstrahlung, and galactic cosmic ray intensities. The Ez should be studied extensively because it not only reveals the variation in the atmosphere [4,5], but it can also be influenced by geological tectonic activities [6,7] and solar activities [8]. Low-latitude generators (mainly mid-latitude and low-latitude thunderstorms) and high-latitude generators (ionosphere–magnetosphere) have a significant impact on magnetic disturbances [9,10]. Importantly, we must avoid the influence of weather on the Ez and only use Ez data obtained under "fair weather" conditions when considering the influence of other factors on the Ez.

The Ez is a key component of the global electric circuit (GEC), which is the large-scale electrical system that encompasses the Earth's surface, the atmosphere, and the ionosphere. The GEC is maintained by the constant movement of electric charges, largely driven by thunderstorms and electrified clouds, which act as generators. The Ez component refers to

the electric field between the Earth's surface and the ionosphere, and under fair weather conditions, it is typically oriented from the ionosphere towards the Earth, with a potential difference of around 250 kV. This potential gradient is influenced by the total column resistance, atmospheric conductivity, and ionization processes. The near-surface Ez is usually around 120 V/m under undisturbed conditions [11]. The Ez is an important diagnostic tool for studying the coupling between the lower atmosphere and space weather phenomena. The GEC provides a framework for understanding how electric fields are maintained and how different layers of the atmosphere are connected electrically. Variations in the Ez offer insight into the dynamic processes occurring in both the atmosphere and the ionosphere.

Magnetic storms, which are caused by the interaction between the solar wind and the Earth's magnetosphere, can significantly alter the structure of the GEC and modify the behavior of the Ez. These storms are typically driven by interplanetary coronal mass ejections (ICMEs) or high-speed solar wind streams, which disturb the magnetosphere and ionosphere [12]. Magnetic storms are classified by indices such as the Dst and Kp index, which measure the intensity of geomagnetic disturbances. The Dst index, which we use in this study, measures the global ring current and is typically used to classify storm intensity into categories: $-50 < \text{Dst} \leq -30$ nT for small storms, $-100 < \text{Dst} \leq -50$ nT for medium storms, $-200 < \text{Dst} \leq -100$ nT for large storms, and $\text{Dst} \leq -200$ nT for super storms [13]. During these geomagnetic storms, solar wind-driven electric fields penetrate into the ionosphere, inducing changes in the atmospheric electric field, including in the Ez. The coupling between the magnetosphere and the lower atmosphere during such disturbances is still a subject of ongoing research, but the influence of ionospheric electric potential and air–ground current variations on the Ez has been observed in several cases [14,15]. Understanding these interactions is crucial, as they may help elucidate broader space weather impacts on Earth's atmosphere. Most researchers have focused on solar activities that may have a considerable impact on global circuits in polar regions [16,17] because polar regions rarely experience anthropogenic pollution and the majority of regions are covered by ice [18]. However, for mid latitudes and low latitudes, atmospheric ionization can be disturbed by terrestrial radioactive elements [19] and the Ez can be highly influenced by local turbulence [20]. Due to the complexity of various factors affecting these measurements, the statistical results of these correlations have not been thoroughly established at mid latitudes and low latitudes [21]. As such, this paper mainly focuses on the variation in the Ez during a mega-magnetic storm at mid latitudes and low latitudes in 2023.

To explore the coupling effect of the solar wind-magnetosphere with the atmospheric electric field, Qiu et al. [22] counted 15 cases of magnetic storms based on extensive observations at the Mohe station (122.36° E, 53.48° N) of the Chinese Meridian Project. For these cases, Mohe was under fair weather conditions throughout the storm period. They showed that the Ez presents a large negative perturbation with a magnitude of approximately 100–600 V/m when the vertical component of the interplanetary magnetic field turns southward. The Ez and solar wind proton number density also tend to change at the same time. Furthermore, Anisimov et al. [23] studied the response of mid-latitude near-Earth Ez variations to strong magnetic storms based on long-term observations of Ezs and geomagnetic fields at the mid-latitude Borok Geophysical Observatory. Then, they collected 19 strong magnetic storm events with a minimal Dst index of <-100 nT and a maximal index value of Kp > 7 for the period 1998–2015. The results showed that the effects of strong magnetic storms on changes in Ez are more effectively manifested around noon during the day and it was characterized by an increase in the Ez value over a time interval of ± 4 h relative to the time of minimum Dst during the strong magnetic storm. Moreover, electric field strength and atmospheric pressure variation field observations in GPhO "Mikhnevo" during a powerful magnetic storm from 17 to 18 March 2015, were investigated by Krasheninnikov et al. [24], who showed that the atmospheric pressure intensity was higher by an order of magnitude than that in quiet conditions and that the electric field strength decreased during the period of maximum auroral activity. In

addition, Ez variations at the mid-latitude station Swider (near Warsaw) have been studied during 14 magnetic storms by Kleimenova et al. [20]. They compared these observed results with the measurements at the polar station Hornsund (Spitsbergen) and showed that the substorm-related Ez disturbances were positive (the Ez values increase) in the local morning and negative (the Ez values decrease) in the local evening. These different Ez deviations depend on the station location relative to the position of the positive or negative plasma convection cells in the polar ionosphere at auroral latitudes. Then, at mid-latitudes, a short daytime negative Ez deviation has been found, which is associated with nocturnal magnetic substorms that develop during the main phase of the magnetic storm [9]. The Ez deviation may be a consequence of the increase in the general ionospheric conductivity caused by the high-energy electron precipitation of the substorm, and another possible cause may be related to the penetration of the storm-related interplanetary electric field into the magnetosphere–ionosphere–atmosphere system.

In this research, based on 167 stations in the near-surface atmospheric electrostatic monitoring network constructed in China, we first exclude the interference of meteorological conditions and data loss, and then we study and analyze the different anomalous signals of Ez from different stations during the mega-magnetic storm that occurred on 24 April 2023. These stations are distributed at different latitudes (mid latitudes and low latitudes). Finally, the variations in Ez at different latitude stations during this mega-magnetic storm are summarized and analyzed.

2. Data and Observations

To study the characteristics of the atmospheric electrostatic environment in different regions and the modulation of the Ez by geological tectonic activities and solar activities, 167 Ez observation stations have been established in Antarctica, Brazil, and China. Their geographical distribution map is shown in Figure 1, and they are not evenly distributed, with 165 stations in China, 1 station in Antarctica, and 1 station in Brazil. Another Ez observation station in the Arctic will also be considered soon. Based on Figure 1, it is evident that these stations are mainly distributed in southeastern and northeastern China due to the sparser population distribution in western China. This network is part of a larger initiative under China's Meridian Project, which monitors space weather and ionospheric activity across multiple stations. Data from some of the Meridian Project stations can be accessed publicly through the Meridian Project Data Center (https://data.meridianproject.ac.cn/, accessed on 24 October 2024). Although the network is still being expanded, and not all station data are available, this offers a valuable resource for researchers interested in studying space weather effects in the Asian sector. In the future, we expect that the availability of data will continue to grow, enhancing opportunities for collaboration and large-scale investigations.

The Ez observations at these stations are made using an electric field mill (EFM), which was made in China, as shown in Figure 2, which is composed of an Ez probe, a digital transmission antenna, an electronics box, a base, a solar power panel and a support rod. For the Ez probe, it is composed of a stator and rotor (the stator and rotor are two sets of similarly fan-shaped metal conductive sheets). When the meter operates, the stator is fixed and grounded while the rotor rotates at a uniform speed; and then, the stator is periodically and alternately exposed to the environmental electric field, which generates induced charges and induced current on its fan blades. The EFM-100 used in the Ez observations has a measurement range of $\pm$50 kV/m, measurement accuracy < 5%, and resolution of 10 V/m [18].



Figure 1. Geographical distribution map of 167 stations of the Ez ground-based monitoring network (the upper left and right corners represent the Brazilian and Antarctic stations, respectively).

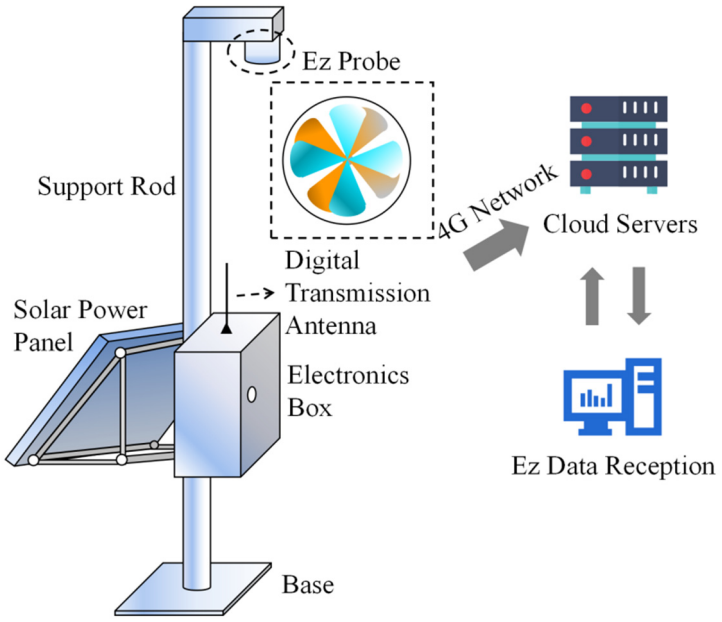

Figure 2. Schematic diagram of EFM-100 instrument operation.

A super geomagnetic storm occurred on 23–24 April 2023, which significantly impacted the GEC and caused noticeable variations in the Ez across multiple stations. This storm was triggered by an interplanetary coronal mass ejection (ICME), a large eruption of solar wind and magnetic fields from the Sun's corona following an M-class solar flare. As the ICME reached Earth, it interacted with the planet's magnetosphere, leading to an

intense geomagnetic disturbance characterized by a Dst index reaching −212 nT. The effects of this storm were notable in several ways. Firstly, it caused substantial perturbations in the electric configuration of the equatorial ionosphere, as well as intense geomagnetically induced currents (GICs) at high latitudes [25,26]. These disturbances were particularly significant during the night, highlighting the global impact of the storm on both high-latitude and mid-latitude regions. The analysis of this event provides a unique opportunity to study the coupling between the magnetosphere and atmosphere, especially in the context of atmospheric electric field disturbances at different latitudes. Our study focuses on analyzing the Ez anomalies at various stations during this geomagnetic storm, aiming to contribute to the broader understanding of space weather impacts on atmospheric electricity.

And the variations in the relevant physical parameters before and after the mega-magnetic storm from 14 to 25 April 2023 (https://omniweb.gsfc.nasa.gov/form/dx1.html, accessed on 24 October 2024) are shown in Figure 3. Panels (a)–(e) represent the Dst index in nT, dawn–dusk electric field Ey in mV/m, solar wind speed V in km/s, its north–south component Bz in nT, and interplanetary magnetic field (IMF) in nT, respectively. The time resolution of all physical parameters in Figure 3 was 1 h. During 14–25 April 2023, a shock associated with the ICME of the interval arrived at 17:00 UT on 23 April, which is shown as the first red line in Figure 3. This shock signature was evident in the IMF, Bz, V, Ey, and Dst indices, and they all showed a sudden increase or decrease around the same time. The sheath region followed this shock until approximately 01:00 UT on 24 April, which is shown as the red shaded part, and then, the ICME ejecta arrived. The ICME lasted until 19:00 UT on the 24th, which is shown in the light blue area in Figure 3. It is important to note that during the period from 15 to 25 April 2023, the galactic cosmic ray (GCR) intensity did not show any significant variation.

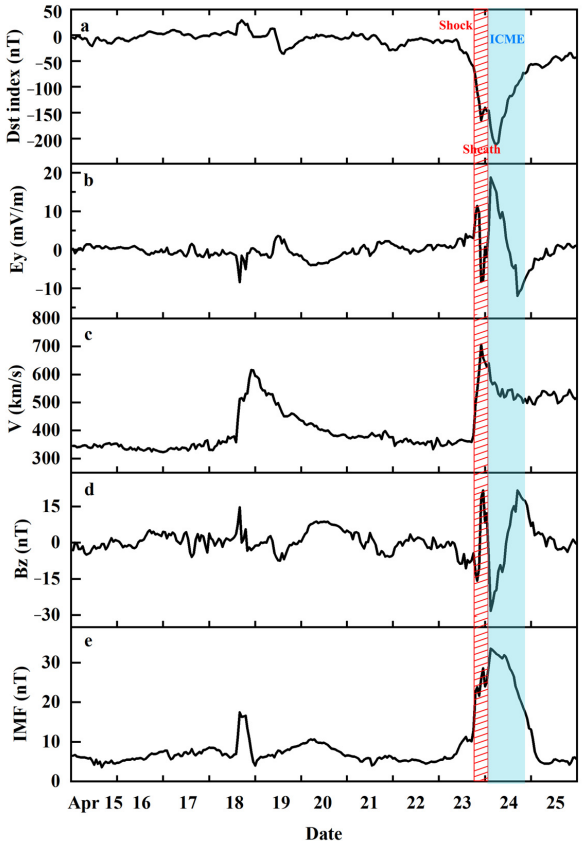

Figure 3. Variation in the Dst index (panel (**a**), nT), dawn–dusk electric field Ey (panel (**b**), mV/m), solar wind velocity V (panel (**c**), km/s), north–south component of the interplanetary magnetic field Bz (panel (**d**), nT), and interplanetary magnetic field magnitude IMF (panel (**e**), nT) during the period of 14–25 April 2023 (time resolution of all physical parameters was 1 h).

To study the alteration of the atmospheric electrostatic environment during this super storm, the Ez values of all 167 stations of the monitoring network were analyzed. There was a loss of Ez data of 8 stations and there were 49 stations with data communication interruptions on 24 April, so they should be excluded. Due to the effect of meteorological conditions, other datasets of 102 stations should also be excluded, and the Ez was finally selected from only 8 stations on April 24th. Harrison and Nicoll [27] summarized the clear-sky criteria that apply to the atmospheric electricity measurements that we used in this study: (1) maximum relative humidity cannot exceed 95%; (2) average wind speed ranged from 1 to 7 m/s; (3) minimum visibility exceeded 10 km; (4) precipitation always remained at 0 mm; and (5) the 10 min average of Ez should be in the range of 0 to 1000 V/m. An additional criterion has been added for the selection of the variation range of the Ez since we do not have access to detailed cloud data.

3. Results

All the Ez data obtained from these observation stations have a time resolution of 1 s. To make the trend of signal changes more apparent, we applied a 10 min sliding average to the raw data before conducting the analysis and comparison. Different altitudes of different stations can cause an Ez enlargement effect and this should be removed. Based on the comparison of our observations in Tibet and Beijing, the station in Tibet is 4000 m higher than that in Beijing, which corresponds to a value of Ez 1.73 times higher than that in Beijing. Moreover, based on the "boundary layer effect" [28] and other observations [29], the variation in the Ez at altitudes below 4000 m can be considered linear, so we adopt the formula $Ez = -0.0002 \times h \times E0 + E0$ (h indicates the altitude in units of m and E0 is raw data in V/m). Then, we compared them with both the mean value of the Ez curve for the day and the fluctuation amplitude of the anomalous curve to clearly describe the magnitude of Ez changes under geomagnetic storms. Therefore, each case resulted in two fluctuation amplitudes. During this super storm, the effects of the storm on the Ez varied among the eight different stations. The geomagnetic storm caused a significant decrease in the Ez at some stations and a noticeable increase at others. We present the Ez curves observed at two representative stations in Figure 4 to illustrate this phenomenon. To enhance the clarity of the comparison results, we plotted them along with the Dst curve in the same graph, as shown in Figure 4. The two Ez observation stations are Ganjingzi Station (GJZ, 121.7° E, 39.0° N) and Jinpuxin Station (JPX, 121.5° E, 38.6° N), with a distance of 47.7 km between them. In Figure 4a, the pink portion represents the intervals where Dst ≤ -200 nT and the green line represents the minimum Dst value of -212 nT, which occurred at 06:00 UT on 24 April 2023. Figure 4b,c display the Ez variations at JPX Station and GJZ Station, respectively, on 24 April. The pink curves represent the raw data, while the blue curves depict the Ez variations after applying a 10 min sliding average. The green sections indicate the Ez variation for all undisturbed fair days in April 2023, with the top and bottom corresponding to 10% and 90% of Ez values, and the orange curves are the average Ez curves. The blue and red arrows indicate the sunset and sunrise times, which were at 02:37 UT and 13:04 UT, respectively.

Based on the results shown in Figure 4, within a 3 h period when Dst ≤ -200 nT, the effects of the storm on Ez variations were significantly different, even though the distance between the stations was only 47.7 km. Regarding their sliding averaged curves, the Ez curve at JPX Station first decreased by approximately 200 V/m at 04:00 UT and then started to increase at 05:00 UT, reaching a maximum of approximately 600 V/m with an increase of approximately 400 V/m. Over the next few hours, it slowly decreased back to normal levels, taking more than 4 h for the decline process. Throughout the entire process, the Ez increased by 260 V/m based on the daily mean variation value, and the time corresponding to the minimum Dst value aligned closely with the maximum Ez value at JPX Station. On the other hand, for station GJZ, the impact of the storm on the Ez variations was notably different. After 0.5 h from the occurrence of the minimum Dst value, the Ez experienced a significant decrease of approximately 50 V/m, followed by a continuous descent. Finally,

it reached a minimum value of approximately −100 V/m at 9:16 UT. Throughout this process, the Ez decreased by 110 V/m based on the daily mean variation. The time of the minimum Ez value at GJZ Station lagged behind the minimum Dst value by 3.3 h. Additionally, both Ez curves experienced varying degrees of disturbance after sunrise and sunset, which verifies the sunrise and sunset effects. Comparing their curves with the background variation of Ez on fair days in April 2023 without perturbation, the effect of such super storms on the increases and decreases in the Ez is more clear.

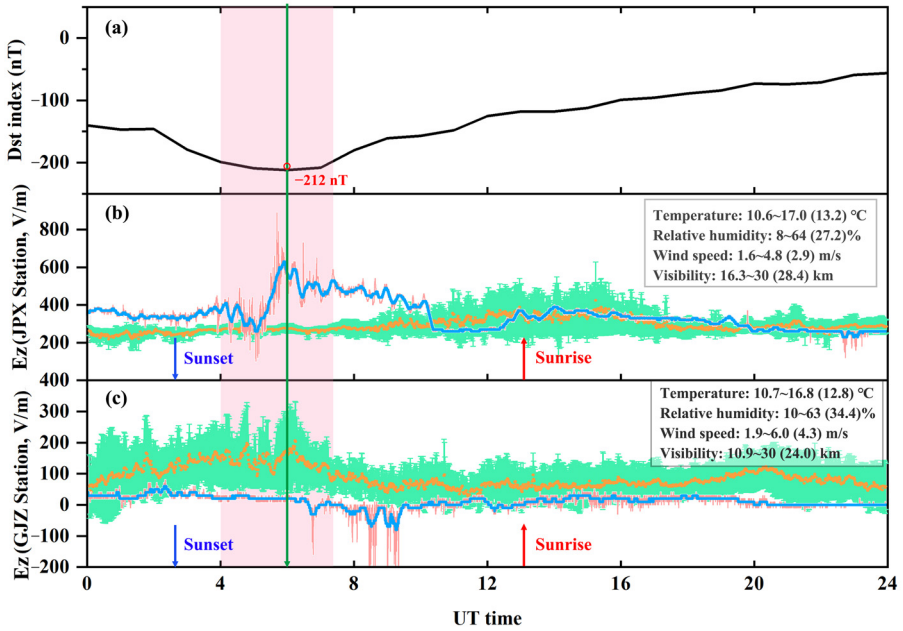

Figure 4. Variation in the Dst index (panel (**a**), nT) and Ez at JPX Station (panel (**b**), V/m) and GJZ Station (panel (**c**), V/m) on 24 April 2023 (the pink part is for Dst ≤ -200 nT and the green vertical line is the minimum Dst; then, the pink curves in panels (**b**,**c**) are the raw data, while the blue line indicates the results after 10 min sliding average processing. And the green sections indicate the Ez variation for all undisturbed fair days in April 2023, with the top and bottom corresponding to 10% and 90% of Ez values, and the orange curves are the average Ez curves. Then, the data in the gray boxes are the ranges of the meteorological parameter variations and those inside brackets are the average values).

During this super geomagnetic storm, the magnitudes of Ez anomalies at eight mid-latitude and low-latitude stations were analyzed, and the results are shown in Figure 5. The background of Figure 5 consists of two latitude–longitude grids (black dashed lines—geographic grid, blue dashed lines—geomagnetic grid), which facilitate the comparison of different station responses to the storm at various locations. The black latitude–longitude coordinates represent geographic coordinates, while the blue latitude–longitude coordinates represent geomagnetic coordinates. To make the identification of different stations clearer, we used different numbered triangles to indicate the locations of these eight stations (1—Jinning Station, 2—Luliang Station, 3—Meiluotai Station, 4—Ali Station, 5—JPX Station, 6—Jinzhou Station, 7—GJZ Station, and 8—Wafangdian Station). The right panel is an enlargement of the red area on the left. Notably, the Ez variations at these stations during the mega-geomagnetic storm are indicated by red arrows (Ez increase) and blue arrows (Ez decrease), and their magnitudes are described by two values. The first value represents the magnitude of variation based on the daily mean value, while the second value represents the magnitude of Ez variation during the storm's anomalous periods.

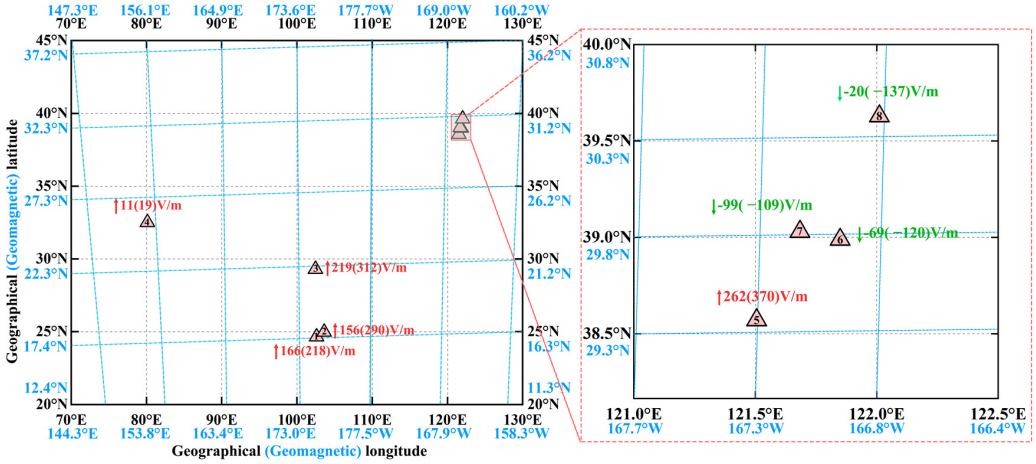

Figure 5. Analysis of Ez anomalous variations at 8 mid-latitude and low-latitude stations during the mega-geomagnetic storm. (Different numbered triangles indicate the locations of these stations (1—Jinning Station, 2—Luliang Station, 3—Meiluotai Station, 4—Ali Station, 5—JPX Station, 6—Jinzhou Station, 7—GJZ Station, and 8—Wafangdian Station). The black and blue grids indicate geographic and geomagnetic latitudes and longitudes, respectively. And Ez variation magnitudes are shown relative to the daily average (first value) and during anomalous periods (second value).

Based on the results shown in Figure 5, during this mega-geomagnetic storm, the magnitudes of Ez variations at these eight stations ranged from 20 to 370 V/m, and the variations based on the daily mean value ranged from 10 to 260 V/m. The increased Ez values at four stations exceeded 200 V/m, and two stations recorded Ez increases exceeding 300 V/m, accounting for 20% of the total. Among them, five stations observed Ez increases, accounting for 62.5% of the total, while only three stations in close proximity recorded Ez decreases. In comparison, the magnitude of Ez increase is approximately 100 V/m larger than the magnitude of Ez decrease. The three stations that experienced an Ez decrease showed similar magnitudes, ranging from 110 to 140 V/m, with variations based on the daily mean falling between 20 and 100 V/m, which is related to their proximity in latitude. Overall, as the geomagnetic latitude increases from 10° N to 35° N, the observed Ez variations are larger at low-latitude stations. Most stations observed Ez increases, except for the three stations near 30° N geomagnetic latitude where Ez decreases were observed. This finding may be related to different underlying physical mechanisms causing their anomalous variations, which will be discussed in more detail later. In terms of longitude, stations in the eastern region observed larger Ez variations compared to the western region, although there is only one station in the west, which is insufficient to draw a conclusion.

To provide a more detailed presentation of our results, the magnitudes of variations and the time differences between them and the Dst index changes for the eight observation cases are depicted in Figure 6. The vertical axis on the left in Figure 6 represents the magnitude of the electric field in units of V/m, and the horizontal axis is the station number, which is the same as the identification in Figure 5. The red bars indicate the amplitude of Ez relative to the daily mean variation value, while the yellow bars represent the Ez variation during anomalous periods. The green bars represent the three cases with decreasing Ez. The vertical axis on the right represents the time differences, which refer to the time interval between the occurrence of the extreme values of Ez associated with the geomagnetic storm and the minimum value of Dst. A positive value of Δt indicates that the extreme value of Ez is delayed by the minimum value of Dst. In Figure 6, the time differences range from 0 to 5.3 h and they are all 0 or positive (indicating that the extreme values of Ez anomalies occur with or after the minimum value of Dst). Only one station had a time difference of 0 h, meaning that the extreme value of Ez coincides with the minimum value of Dst, indicating synchronous changes. Furthermore, the time differences between the Ez and Dst variations are longer in low-latitude regions than in mid-latitude regions.

This finding suggests that it takes more time for the effects of the same geomagnetic storm to impact the Ez in low-latitude regions. Based on the results depicted in Figure 6, the time differences between the Ez and Dst variations have a nonlinear relationship with the magnitude of the Ez variations.

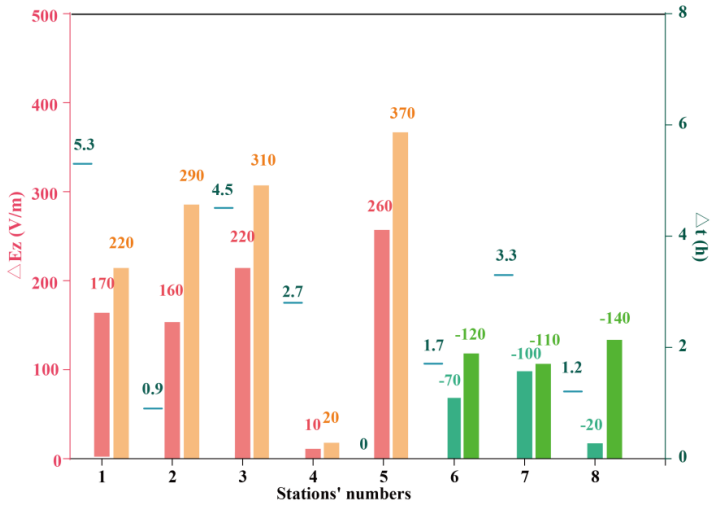

Figure 6. Results of Ez variation magnitude and time difference with Dst index during the mega-geomagnetic storm. (The left vertical axis represents the Ez variation magnitude in V/m, with red bars indicating Ez magnitudes relative to the daily average and yellow bars representing Ez variation magnitudes during anomalous periods. The green bars represent the three cases of Ez decreases, and the right vertical axis represents the time difference between the Ez extreme value and the minimum Dst).

4. Discussion

Further discussions considered the different observations of Ez increases or decreases among stations during the same geomagnetic storm. During a super storm, the intensity of galactic cosmic rays decreases due to the Forbush effect, which is one of the main sources of ionization in the surface layer. Then, the near-surface conductivity decreases, and the Ez increases. For the observed Ez decrease, it is possible that only the atmospheric conductivity at high altitudes decreased, and then the air–earth current and the Ez decreased. The precise differentiation of the underlying physical mechanisms requires further investigations and the integration of observations from other physical parameters, which will be duly considered in future research.

The horizontal inhomogeneity of the vertical atmospheric electric field (Ez) observed in Figure 5 is particularly intriguing and deserves further analysis. One possible explanation for this non-uniformity is the presence of horizontal potential differences between ionospheric regions at different latitudes and longitudes. These differences arise due to variations in the ionospheric electric potential, which are influenced by factors such as geomagnetic latitude, solar activity, and local atmospheric conditions. At different latitudes, the ionosphere experiences uneven electric potentials due to the differential effects of solar radiation and geomagnetic activity. This creates horizontal potential gradients across regions, leading to differences in the electric fields observed at the Earth's surface. Specifically, the observed inhomogeneities in the Ez may result from the spatial variations in the air–ground current, which are driven by these ionospheric potential differences. These gradients cause the electric field to vary horizontally, contributing to the distinct Ez anomalies we recorded at different stations.

This study provides valuable insights into the behavior of the Ez during a super geomagnetic storm. However, there are a few limitations to consider. Firstly, the analysis is based on data from a single geomagnetic storm event, which may not fully capture the variability of Ez responses to different types of storms or under varying conditions.

Additionally, the spatial coverage of the observation stations is concentrated primarily in China, with only a few stations in other regions. This may limit the generalizability of the findings to other geographic areas.

The influence of solar activity on the global atmospheric electric circuit is well established, but the effects at mid-latitudes and low latitudes pose challenges for researchers. These challenges primarily include the difficulty of accurately isolating turbulent fluctuations and sporadic influences on atmospheric electric fields from local weather conditions, anthropogenic impacts, and geological activities [29]. Additionally, the electrical signal transmitted through the lower atmosphere also affects measurements [20]. In future observational studies, it will be essential to incorporate other observed parameters related to the atmosphere and ionosphere at the same observation stations, such as radon concentration, atmospheric conductivity, displacement current, ionospheric potential, and gas emissions. These additional parameters will greatly contribute to our understanding of the underlying physical mechanisms and uncover the truth behind Ez variations.

5. Conclusions

In this study, we conducted an analysis of the anomalous variations in Ez observed at eight observation stations located at mid latitudes and low latitudes during the mega-geomagnetic storm on 24 April 2023. The following conclusions and discussions were obtained as a result of this study:

Super geomagnetic storms have a significant impact on global atmospheric electricity. The observed variations in Ez associated with this super geomagnetic storm ranged from 20 to 370 V/m. The range of variations relative to the daily mean Ez was within 10 to 260 V/m. The extreme values of Ez anomalies occurred with a time delay of 0 to 5.3 h after the minimum Dst value. Only one station observed Ez anomalies that were synchronous with Dst variations.

During this mega-geomagnetic storm, five stations observed an increase in Ez, while three stations observed a decrease. They both appear in the afternoon local time, a difference that is clearly different from Kleimenova et al. [20]. This discrepancy in the observed Ez variations may be attributed to different underlying physical mechanisms causing the anomalies. Notably, the three stations with an Ez decrease were in close proximity, near a geomagnetic latitude of 30° N. The magnitude of the decrease in Ez was similar for these stations, ranging from 110 to 140 V/m.

Author Contributions: W.L. processed and analyzed the data, prepared the original draft with contributions from all authors. Z.S., Z.Y., T.C., Q.X., J.L. and Z.M. were responsible for the discussions. All authors have read and agreed to the published version of the manuscript.

Funding: This research was supported by the National Key R&D Program of China (Nos. 2023YFC2604900, 2023YFC2604904, 2023YFF0719800 and 2023YFF0719801).

Institutional Review Board Statement: Not applicable.

Informed Consent Statement: Not applicable.

Data Availability Statement: The datasets used or analyzed during the current study are available from the corresponding author on reasonable request. The data are not publicly available due to privacy.

Acknowledgments: The authors appreciate those who were involved in the atmospheric electric field observations.

Conflicts of Interest: The authors declare that they have no competing interests.

References

1. Williams, E.R. The global electrical circuit: A review. *Atmos. Res.* **2009**, *91*, 140–152. [CrossRef]
2. Williams, E.; Mareev, E. Recent progress on the global electrical circuit. *Atmos. Res.* **2014**, *135–136*, 208–227. [CrossRef]
3. Krasheninnikov, A.V.; Loktev, D.N.; Soloviev, S.P. Megacity aerosol pollution and atmospheric electric field disturbances. *Izv. Atmos. Ocean. Phys.* **2020**, *56*, 759–772. [CrossRef]

4. Yair, Y.; Yaniv, R. The effects of fog on the atmospheric electrical field close to the surface. *Atmosphere* **2023**, *14*, 549. [CrossRef]
5. Smirnov, S. Association of the negative anomalies of the quasistatic electric field in atmosphere with Kamchatka seismicity. *Nat. Hazards Earth Syst. Sci.* **2008**, *8*, 745–749. [CrossRef]
6. Choudhury, A.; Guha, A.; De, B.; Roy, R. A statistical study on precursory effects of earthquakes observed through the atmospheric vertical electric field in northeast India. *Ann. Geophys.* **2013**, *56*, R0331. [CrossRef]
7. Nicoll, K.A. Space weather influences on atmospheric electricity. *Weather* **2014**, *69*, 238–241. [CrossRef]
8. Kleimenova, N.G.; Kozyreva, O.V.; Michnowski, S.; Kubicki, M. Effect of magnetic storms in variations in the atmospheric electric field at midlatitudes. *Geomagn. Aeron.* **2008**, *48*, 622–630. [CrossRef]
9. Rycroft, M.J.; Nicoll, K.A.; Aplin, K.L.; Harrison, R.G. Recent advances in global electric circuit coupling between the space environment and the troposphere. *J. Atmos. Sol. Terr. Phys.* **2012**, *90–91*, 198–211. [CrossRef]
10. Mayer, D.; Stork, M. Indicator of the influence of a geomagnetic storm on the transmission electric system. *J. Electr. Eng.* **2023**, *74*, 32–39. [CrossRef]
11. Nicoll, K.A. Measurements of atmospheric electricity aloft. *Surv. Geophys.* **2012**, *33*, 991–1057. [CrossRef]
12. Chen, Z.L. *Theoretical Modeling of Low-Frequency Radar Signal Propagation Characteristics in the Outer Radiation Belt of the Earth*; Nanchang University: Nanchang, China, 2022.
13. Corney, R.C.; Burns, G.B.; Michael, K.; Frank-Kamenetsky, A.V.; Troshichev, O.A.; Bering, E.A.; Papitashvili, V.O.; Breed, A.M.; Duldig, M.L. The influence of polar-cap convection on the geoelectric field at Vostok, Antarctica. *J. Atmos. Sol. Terr. Phys.* **2003**, *65*, 345–354. [CrossRef]
14. Liu, J.; Zhang, D.; Hao, Y.; Xiao, Z. The time delay between the equatorial ionization anomaly and the equatorial electrojet in the eastern Asian and American sectors. *Adv. Space Res.* **2022**, *69*, 187–196. [CrossRef]
15. Ren, D.; Lei, J.; Zhou, S.; Li, W.; Huang, F.; Luan, X.; Dang, T.; Liu, Y. High-speed solar wind imprints on the ionosphere during the recovery phase of the August 2018 geomagnetic storm. *Space Weather* **2020**, *18*, e2020SW002480. [CrossRef]
16. Frank-Kamenetskii, A.V.; Kotikov, A.L.; Kruglov, A.A.; Burns, G.B.; Kleimenova, N.G.; Kozyreva, O.V.; Kubitski, M.; Odzimek, A. Variations in the near-surface atmospheric electric field at high latitudes and ionospheric potential during geomagnetic perturbations. *Geomagn. Aeron.* **2012**, *52*, 629–638. [CrossRef]
17. Li, L.; Chen, T.; Ti, S.; Wang, S.H.; Song, J.J.; Cai, C.L.; Liu, Y.H.; Li, W.; Luo, J. Fair-weather near-surface atmospheric electric field measurements at the Zhongshan Chinese Station in Antarctica. *Appl. Sci.* **2022**, *12*, 9248. [CrossRef]
18. Chen, T.; Li, L.; Zhang, X.; Wang, C.; Jin, X.; Wu, H.; Ti, S.; Wang, S.; Song, J.; Li, W.; et al. Possible locking shock time in 2–48 hours. *Appl. Sci.* **2023**, *13*, 813. [CrossRef]
19. Kleimenova, N.; Kozyreva, O.; Michnowski, S.; Kubicki, M. Influence of geomagnetic disturbances on atmospheric electric field (Ez) variations at high and middle latitudes. *J. Atmos. Sol. Terr. Phys.* **2013**, *99*, 117–122. [CrossRef]
20. Michnowski, S. Solar wind influences on atmospheric electricity variables in polar regions. *J. Geophys. Res. Atmos.* **1998**, *103*, 13939–13948. [CrossRef]
21. Qiu, S.; Xie, Y.; Shi, M.; Yousof, H.; Soon, W.; Ren, Z.; Jia, M.; Dou, X. Observations and analysis of the mid-latitude atmospheric electric field during geomagnetic activity. *J. Geophys. Res. Space Phys.* **2022**, *127*, e2022JA030785. [CrossRef]
22. Anisimov, S.V.; Shikhova, N.M.; Kleimenova, N.G. Response of a magnetospheric storm in the atmospheric electric field of the midlatitudes. *Geomagn. Aeron.* **2021**, *61*, 180–190. [CrossRef]
23. Despirak, I.; Setsko, P.; Lubchich, A.; Hajra, R.; Sakharov, Y.; Lakhina, G.; Selivanov, V.; Tsurutani, B.T. Geomagnetically induced currents (GICs) during strong geomagnetic activity (storms, substorms, and magnetic pulsations) on 23–24 April 2023. *J. Atmos. Sol. Terr. Phys.* **2024**, *261*, 106293. [CrossRef]
24. Juusola, L.; Vanhamäki, H.; Viljanen, A.; Smirnov, M. Induced currents due to 3D ground conductivity play a major role in the interpretation of geomagnetic variations. *Ann. Geophys.* **2020**, *38*, 983–998. [CrossRef]
25. Krasheninnikov, A.; Soloviev, S.; Rybnov, Y.; Solovyov, A. Atmospheric pressure and electric field variations during auroras. In Proceedings of the Russian Open Conference on Radio Wave Propagation (RWP), Kazan, Russia, 1–6 July 2019; IEEE: Piscataway, NJ, USA, 2019; pp. 548–551.
26. Harrison, R.G.; Nicoll, K.A. Fair weather criteria for atmospheric electricity measurements. *J. Atmos. Sol. Terr. Phys.* **2018**, *179*, 239–250. [CrossRef]
27. Tao, C.; Lei, L.; Wen, L.; Shuo, T.; Han, W.; Shihan, W.; Renkang, L.; Fushan, L.; Huawei, Z.; Hailong, S.; et al. Characteristics of atmospheric electric field variation with height in the Qaidam Basin, Qinghai Province. *Chin. J. Space Sci.* **2021**, *41*, 626–634.
28. Zhou, H.; Diendorfer, G.; Thottappillil, R.; Pichler, H. Fair-weather atmospheric electric field measurements at the Gaisberg Mountain in Austria. In Proceedings of the Electromagnetics Research Symposium Proceedings, Marrakesh, Morocco, 20–23 March 2011; Volume 1303.
29. Rycroft, M.J. Electrical processes coupling the atmosphere and ionosphere: An overview. *J. Atmos. Sol. Terr. Phys.* **2006**, *68*, 445–456. [CrossRef]

Disclaimer/Publisher's Note: The statements, opinions and data contained in all publications are solely those of the individual author(s) and contributor(s) and not of MDPI and/or the editor(s). MDPI and/or the editor(s) disclaim responsibility for any injury to people or property resulting from any ideas, methods, instructions or products referred to in the content.